Linear and nonlinear dielectric susceptibilities of disordered lead scandium tantalate

2001 J. Phys.: Condens. Matter 13 5449

(http://iopscience.iop.org/0953-8984/13/23/304)

INSTITUTE OF PHYSICS PUBLISHING JOURNAL OF PHYSICS: CONDENSED MATTER

J. Phys.: Condens. Matter **13** (2001) 5449–5462 www.iop.org/Journals/cm PII: S0953-8984(01)21206-5

Linear and nonlinear dielectric susceptibilities of disordered lead scandium tantalate

Jae-Hyeon Ko[1,3], Fuming Jiang[1], Seiji Kojima[1], T A Shaplygina[2] and S G Lushnikov[2]

[1] Institute of Materials Science, University of Tsukuba, Tsukuba, Ibaraki 305-8573, Japan
[2] A F Ioffe Physical Technical Institute, Russian Academy of Sciences, St Petersburg, 194021, Russia

E-mail: jhko@ims.tsukuba.ac.jp (Jae-Hyeon Ko)

Received 19 January 2001, in final form 19 April 2001

Abstract

The linear and nonlinear complex dielectric constants of the disordered lead scandium tantalate ($Pb(Sc_{1/2}Ta_{1/2})O_3$) relaxor system, which is characterized by B-site disorder, were measured. The linear dielectric susceptibility showed a typical relaxor behaviour which can be described by the Vogel–Fulcher law and an additional weak dispersion which can be observed only at very low frequencies. The temperature dependence of the third-harmonic response also showed a frequency dispersion, and the peak temperatures of the real part obeyed the Vogel–Fulcher law with a freezing temperature close to that of the linear response. The observed nonlinear susceptibility showed a quite similar behaviour to that of lead magnesium niobate ($Pb(Mg_{1/3}Nb_{2/3})O_3$). The temperature variation is discussed on the basis of the theoretical predictions of the spherical random-bond–random-field model (Pirc R and Blinc R 1999 *Phys. Rev.* B **60** 13 470) and a recent phenomenological model (Glazounov A E and Tagantsev A K 2000 *Phys. Rev. Lett.* **85** 2192).

1. Introduction

Relaxor ferroelectrics have attracted great interest for several decades, not only because of their complex dynamical properties but also because of the potential applicability in various fields of industry. Relaxors show several typical behaviours such as a diffusive dielectric response with broad dielectric maxima, the absence of long-range order and persistent local polarizations far above the freezing temperature [1, 2]. Although several theoretical models have been proposed to explain the complex behaviours of relaxors, a detailed microscopic picture for them is not clear yet. The superparaelectric model [1], or its modified version [3], can explain the dynamic behaviour of relaxor ferroelectrics in the high-temperature range above the freezing temperature. The dipolar glass model [4–6], random-field-driven ferroelectric nanodomain

[3] Author to whom any correspondence should be addressed.

0953-8984/01/235449+14$30.00

model [7, 8] and spherical random-bond–random-field model [9–11] have also been suggested and could explain some aspects of the various experimental results. In particular, the question of whether the low-temperature phase of relaxors is due to the frustrated microdomain state driven by local random fields [7, 8] or due to the random, glassy interactions between the polar regions [4–6, 9–11] has been seen as crucial as regards the nature of relaxor ferroelectrics.

Recently, nonlinear dielectric susceptibility has been suggested as a useful physical property as regards testing various models, particularly the spherical random-bond–random-field (SRBRF) model [9–11] and the model of interphase boundary motions of the polar regions [8, 12], which were proposed to explain the dielectric response of relaxors. According to the SRBRF model, $a_3 = \varepsilon_3/\varepsilon_1^4$, where ε_1 and ε_3 are static linear and third-harmonic nonlinear dielectric constants, respectively, should show a sharp peak near the freezing temperature (T_f) in the presence of weak random fields [9]. However, due to the dynamic nature of the conventional dielectric spectroscopy adopted in the experiment, only the high-temperature tail of a_3 could be observed. It showed a dip at a certain temperature far above T_f and an increasing behaviour below that temperature in several relaxor systems [11]. In contrast to this, interphase boundary motions of the polar regions have been suggested as a physical origin of the polarization response of relaxors on the basis of analysis of the measured nonlinearity of $Pb(Mg_{1/3}Nb_{2/3})O_3$ (PMN) as functions of the strength of a DC bias field and an AC probe amplitude [8, 12]. Very recently, a phenomenological model was proposed by the same authors to describe the frequency dispersion of the nonlinear dielectric susceptibility of PMN, from which it was claimed that a frequency-independent nonlinear coefficient corresponding to the static nonlinear dielectric susceptibility was obtained [13]. The derived coefficient was shown to increase with decreasing temperature without representing any peak at the freezing temperature [13], which is in contrast to the theoretical prediction of the SRBRF model. It would thus be very interesting to investigate the nonlinear dielectric response in other relaxor systems to test the suggested models.

$Pb(Sc_{1/2}Ta_{1/2})O_3$ (PST) belongs to the $Pb(B'_{1/2}B''_{1/2})O_3$-type group of perovskite relaxors characterized by B-site disorder. Since the degree of disorder of the B site can be controlled by specific thermal treatments [14–16], PST has been studied as a model system which could reveal the role of the B-site disorder in the relaxor behaviours. Since the pioneering work by Setter and Cross [14], PST has been studied by various experimental methods such as dielectric spectroscopy [14, 16–18, 29], the Raman scattering [19] and x-ray and neutron scattering [20, 21] techniques, TEM and differential scanning calorimetry [22], NMR techniques [23] and IR reflectivity [33, 34]. Early work revealed that the B-site disorder could suppress the ferroelectric phase transition and enhance the relaxor behaviour [14]. The peak temperature and the absolute value of the dielectric constant decreased with the increase of the degree of disorder, as was reconfirmed by Viehland and Li [17]. However, Chu *et al* reported a spontaneous relaxor–ferroelectric transition in fully disordered PST ceramic samples, for the first time [16, 22]. They also observed the same phenomenon in the $Pb(Sc_{1/2}Nb_{1/2})O_3$ (PSN) relaxor system [24]. In view of the fact that there was no spontaneous relaxor–ferroelectric transition in PST samples containing lead vacancies, they suggested that such vacancies could stabilize the relaxor phase without any spontaneous relaxor–ferroelectric transition. In addition to the broad dielectric dispersion of relaxors in the low-frequency range, high-frequency relaxations above 10 MHz were also observed [18, 29, 33, 34]. Since these high-frequency and microwave relaxations comprise the main relaxation mechanism of relaxors at high temperatures [29, 33, 34], their microscopic origins and relations to the relaxor behaviour are a very interesting subject, to be elucidated in the future.

In this study, we will report linear and nonlinear dielectric susceptibilities of disordered PST single crystals. We extended the low-frequency limit of the dielectric study down to 0.1 Hz,

and examined the effects of the thermal cycling and DC bias field on the dielectric property. The third-harmonic component of the nonlinear polarization response was investigated, and the result is discussed in comparison with that for the linear dielectric response and theoretical predictions of the recently developed theoretical models [11, 13].

2. Experiment

PST single crystals were grown by spontaneous crystallization from the solution in the melt. The mixture of polycrystalline PST and PbO–PbF_2–B_2O_3 solvent in the appropriate proportions was sealed in a platinum crucible and then placed into a corundum crucible filled with Al_2O_3. The crucible with the mixture was rapidly raised to 1250 °C, kept at that temperature for four hours and then finally cooled to 900 °C at a rate of 2–3 °C h^{-1}. The maximum size of the crystals obtained was about $3 \times 3 \times 3$ mm^3. The S-parameter representing the degree of B-site order [14] was found to be 0.29 from an x-ray diffraction experiment. Due to there being plenty of lead in the environment, the content of lead vacancies in the single crystal is thought to be minimized. Two plates were cut along the ⟨100⟩ and ⟨110⟩ directions and then polished to optical quality. Silver paste, which was fired at 600 K, was used as an electrode.

The linear dielectric constant was measured either by a Solartron impedance analyser (SI1260) or a digital lock-in amplifier (LI5640, NF Electronic Instruments) from 0.1 Hz to 1 MHz. A current amplifier (Keithley 428) was adopted as a current-to-voltage converter for the Solartron system at low frequencies below 10 Hz. To examine the effect of a DC bias on the dielectric constant, the internal DC bias source of the Solartron was used. Temperature was controlled by a closed-cycle helium refrigerator (RMC LTS-22) and a home-made high-temperature furnace combined with a digitized temperature controller (SI9650/LakeShore331) to cover a temperature range from 400 K down to 100 K. Temperature was monitored either by a silicon diode sensor or a chromel–alumel thermocouple. The cooling or heating rate was 0.5 K min^{-1}.

The third-harmonic nonlinear polarization response was measured by using a digital lock-in amplifier. The sample was connected to a low-loss standard capacitor in series and the voltage across the standard capacitor was picked up by the digital lock-in amplifier [25]. Using the function for detecting the higher-order harmonics of this device, both the linear and the third-harmonic responses could be measured in one temperature scan.

For the dielectric measurements the amplitude of the probe sine wave was always less than 50 V cm^{-1}. Before each of the measurements, the sample was annealed at about 550 K for one hour. Since there was no qualitative difference between the ⟨100⟩ and ⟨110⟩ samples, we will report results for the ⟨100⟩ sample unless stated otherwise.

3. Results and discussion

3.1. Linear dielectric susceptibility

In figure 1, we show the real and imaginary parts of the linear dielectric constant of PST along the ⟨100⟩ axis. It shows the typical dielectric dispersion usually observed in other relaxors such as PMN [1]. The maximum temperatures of both the real and imaginary parts of the complex dielectric constant decrease with the decrease of the probe frequency. This result is consistent with the previous results observed for single-crystal PST samples [14, 17]. Since the absolute value of the dielectric dispersion and the temperature at which it takes place decrease with increasing disorder, the absolute value of the dielectric maximum in the present study is smaller at lower temperature than the results of [14] and [17]. However, our result does

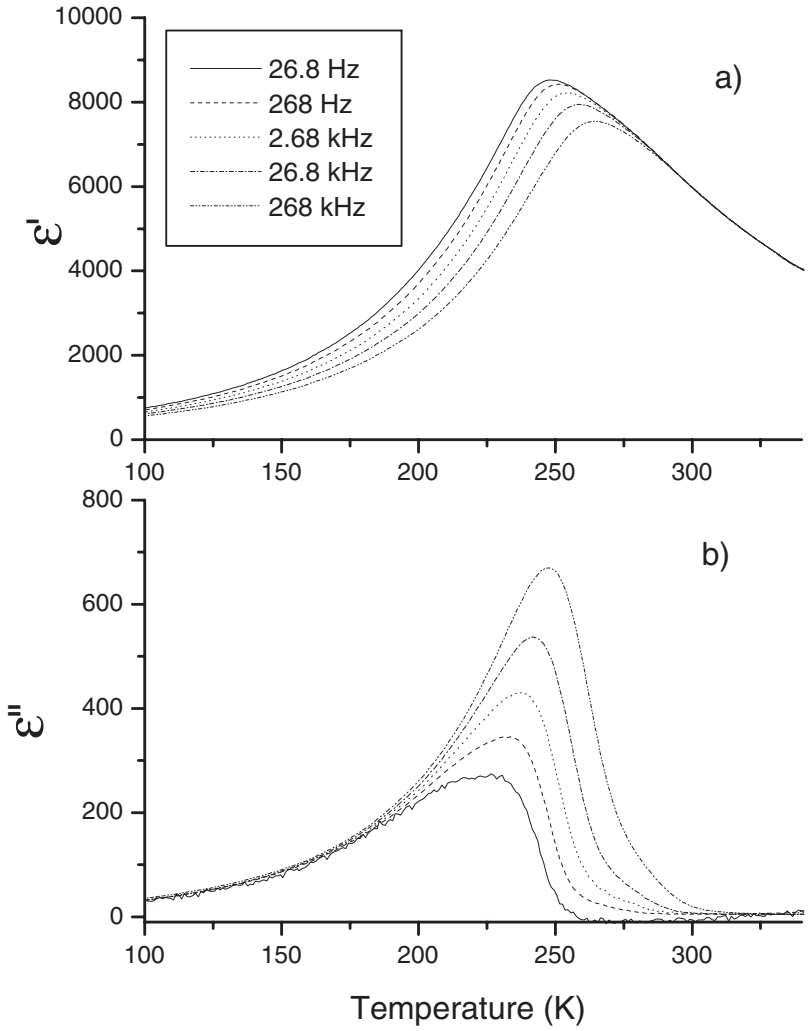

Figure 1. The real part (a) and imaginary part (b) of the complex dielectric constant of PST along the ⟨100⟩ axis at several measurement frequencies as functions of temperature.

not show a spontaneous relaxor–ferroelectric transition which was observed in ceramic PST samples [16]. It is also curious that the absolute value of the dielectric constant increases with increasing degree of B-site order in single-crystal PST samples (references [14, 17] and present work) while it decreases in the case of ceramic samples [16]. The origin of this difference is not clear at present. It is interesting to note that there has been no report of single-crystal PST samples which show a spontaneous relaxor–ferroelectric transition, but we cannot exclude the possibility of a small content of lead vacancies in the single-crystal samples reported on (references [14, 17] and present work) which might suppress a spontaneous relaxor–ferroelectric transition.

The peak temperatures of the dielectric maxima in the real part of the complex dielectric constant follow the phenomenological Vogel–Fulcher law, which can be expressed as

$$\omega = \omega_0 \exp[-E/(T_m - T_f)] \tag{1}$$

where ω and T_m denote a probe angular frequency and the corresponding peak temperature of the real part in the dielectric constant, respectively. ω_0, E and T_f are fitting parameters: an attempt frequency, an activation energy and a freezing temperature, respectively. Figure 2 shows the result of fitting T_m with equation (1) with typical experimental error bars. The parameters obtained are $\tau_0(1/\omega_0) = 5.5 \times 10^{-12}$ s, $E = 409 \pm 53$ K and $T_f = 229 \pm 2$ K. We compared our results with the previous ones [17], as tabulated in table 1. All three parameters show similar orders of magnitude. The freezing temperature T_f decreases and the activation energy increases with the increase of B-site disorder.

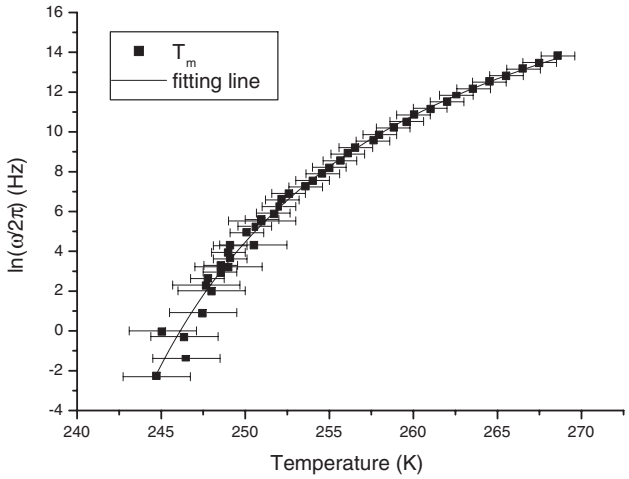

Figure 2. The best-fit result for the maximum temperatures of the real part of the dielectric constant fitted with the Vogel–Fulcher relation (equation (1)) with typical error bars.

Table 1. Best-fit parameters for the maximum temperatures of the real part of the dielectric constant as fitted by equation (1) for the PST single crystal compared with the previously reported results. S is the degree of B-site order determined by x-ray diffraction.

	$S = 0.29$ (present work)	$S = 0.35$ [17]	$S = 0.80$ [17]
$\tau_0(1/\omega_0)$ (s)	5.5×10^{-12}	10^{-12}	10^{-12}
E (K)	409	348	174
T_f (K)	229	233	279

In figure 3, the complex dielectric constants are plotted in the frequency domain from 0.1 Hz to 1 MHz. In the high-temperature range, we can only see the low-frequency tail of the main dielectric dispersion which is above 1 MHz. Several studies have reported the existence of high-frequency relaxations in many perovskite ferroelectrics and ferroelectric relaxors [26, 27] including the ordered and disordered PST samples [18, 29, 33, 34]. For the high-frequency relaxation at around 100 MHz, the relaxation time increases as the temperature approaches the phase transition (or freezing) temperature from the high-temperature side and decreases again with decreasing temperature below the transition (or freezing) temperature [18]. The origin of this high-frequency relaxation in PST relaxors has been ascribed either to the cooperative hopping of Ta^{5+} ions along correlation chains [18] or to the correlated dynamic clusters related to the Pb disorder [29]. In addition to this, an overdamped mode in the 10 cm^{-1} range has been observed in the paraelectric phase which was ascribed to highly anharmonic disordered Pb hopping [34].

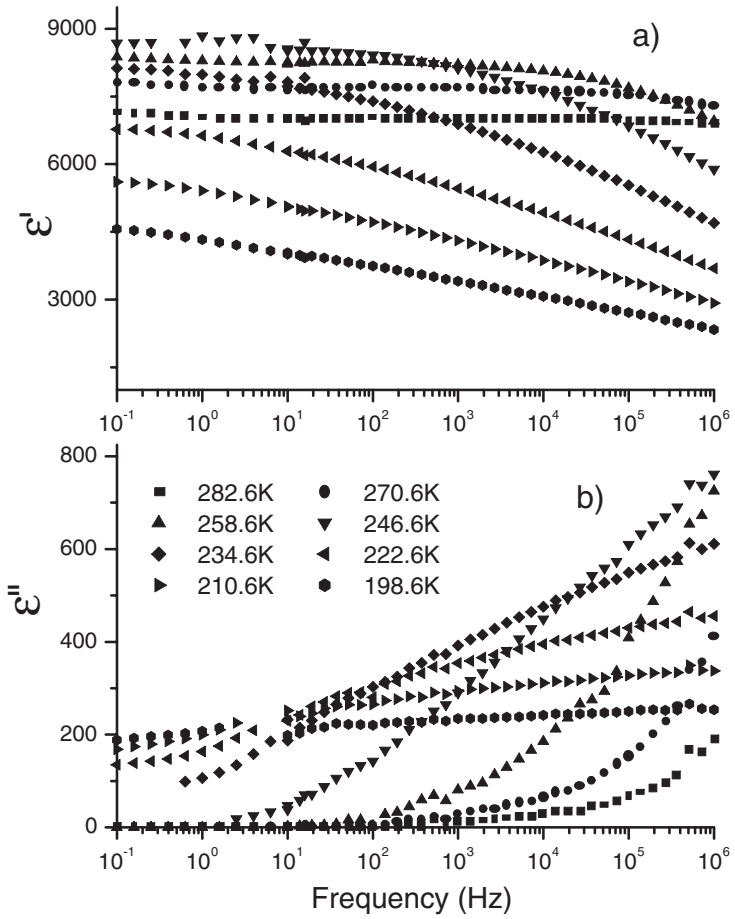

Figure 3. The real part (a) and imaginary part (b) of the complex dielectric constant of PST along the ⟨100⟩ axis at several temperatures as functions of frequency between 0.1 Hz and 1 MHz.

As temperature decreases, the dispersion region approaches our frequency window and the dispersion becomes extremely polydispersive at lower temperatures, which is a typical behaviour for ferroelectric relaxors. At 198.6 K, the imaginary part is nearly flat in our frequency window, corresponding to a very broad distribution of relaxation times. This can also be seen from the Cole–Cole plot which is shown in figure 4. At all of the temperatures in our study, the Cole–Cole plot shows deviations from the semicircle of the simple monodispersive Debye case and becomes quite flat at 190 K, reflecting the fact that the imaginary part of the complex dielectric constant is almost independent of the frequency.

The thermal hysteresis and the effect of a DC bias were also examined. In figure 5(a), the real parts of the dielectric constants measured at 1 kHz during both cooling and heating processes are plotted. Although we can see a slight thermal hysteresis between the two processes, the difference is negligible compared to the one observed in the ceramic samples [16], which showed a spontaneous relaxor–ferroelectric transition of first order. The corresponding imaginary part of the dielectric constant, in the inset of figure 5(a), also shows negligible thermal hysteresis. To examine a the effect of a bias field, we applied a DC bias field of 400 V cm^{-1} to the sample and measured the dielectric constant at the probe frequency of

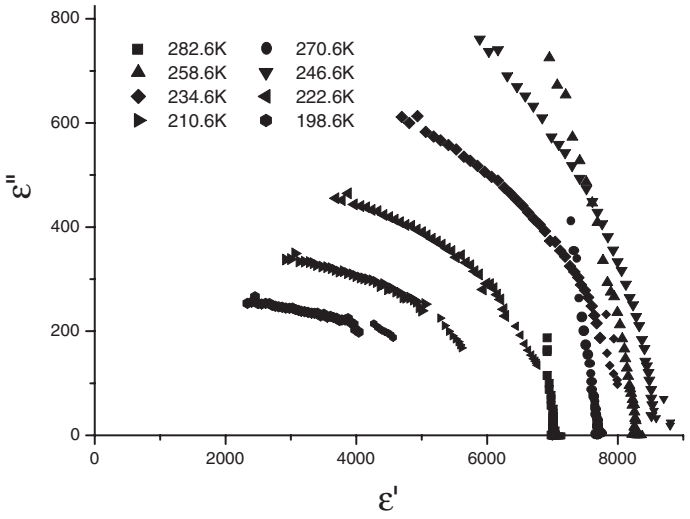

Figure 4. A Cole–Cole plot of the complex dielectric constant of PST at several temperatures.

19.6 kHz during the cooling process; the results are plotted in figure 5(b). The absolute value of the real part of the dielectric constant is reduced by about 5% at high temperatures above the dielectric maximum compared to the one obtained with no bias field. This means that a DC field suppresses the dynamics of the polar nano-regions in this high-temperature range. However, as temperature decreases, the interactions between the polar regions will become stronger and the DC bias field of 400 V cm^{-1} is too small to have any appreciable effect on the dynamics of the polar regions, resulting in there being no difference in the value of the dielectric constant between the two processes at low temperatures.

Before closing this section, we will briefly report a low-frequency dispersion observed in the linear dielectric susceptibility. The complex dielectric constants between 7.5 kHz and 0.75 Hz are shown in figure 6. Comparing these data to those in figure 1, we can clearly see another dielectric dispersion in the high-temperature range above the dielectric maxima, as can be seen from the imaginary part of the dielectric constant. This contribution becomes larger at lower frequencies, which is evident in the inset of figure 6(b). Since this additional weak anomaly has been detected by both the Solartron impedance analyser and the digital lock-in amplifier, it should not be an experimental error. In addition to that in the dielectric data, we could also observe two anomalies in the temperature dependence of the pyroelectric current, one corresponding to the freezing process near the freezing temperature and the other to the second dielectric anomaly in the high-temperature range [28]. As will be shown below, this newly observed dielectric dispersion has some effect on the third-order-harmonic component of the polarization response. However, it is not certain whether it is related to incommensurate modulations in the polar regions [30], or to pre-existing anisotropic antiferroelectric correlations observed in PSN [31] or some other physical origin. Further experiments are ongoing that are designed to reveal the origin of this additional process, and will be reported elsewhere [28].

3.2. Nonlinear dielectric susceptibility

The absolute value of the third-harmonic component of the dielectric response, $|P_3| = \sqrt{(P_3')^2 + (P_3'')^2}$, is plotted in figure 7(a) as functions of temperature and frequency. The absolute value increases and the maximum peak position shifts to lower temperature with

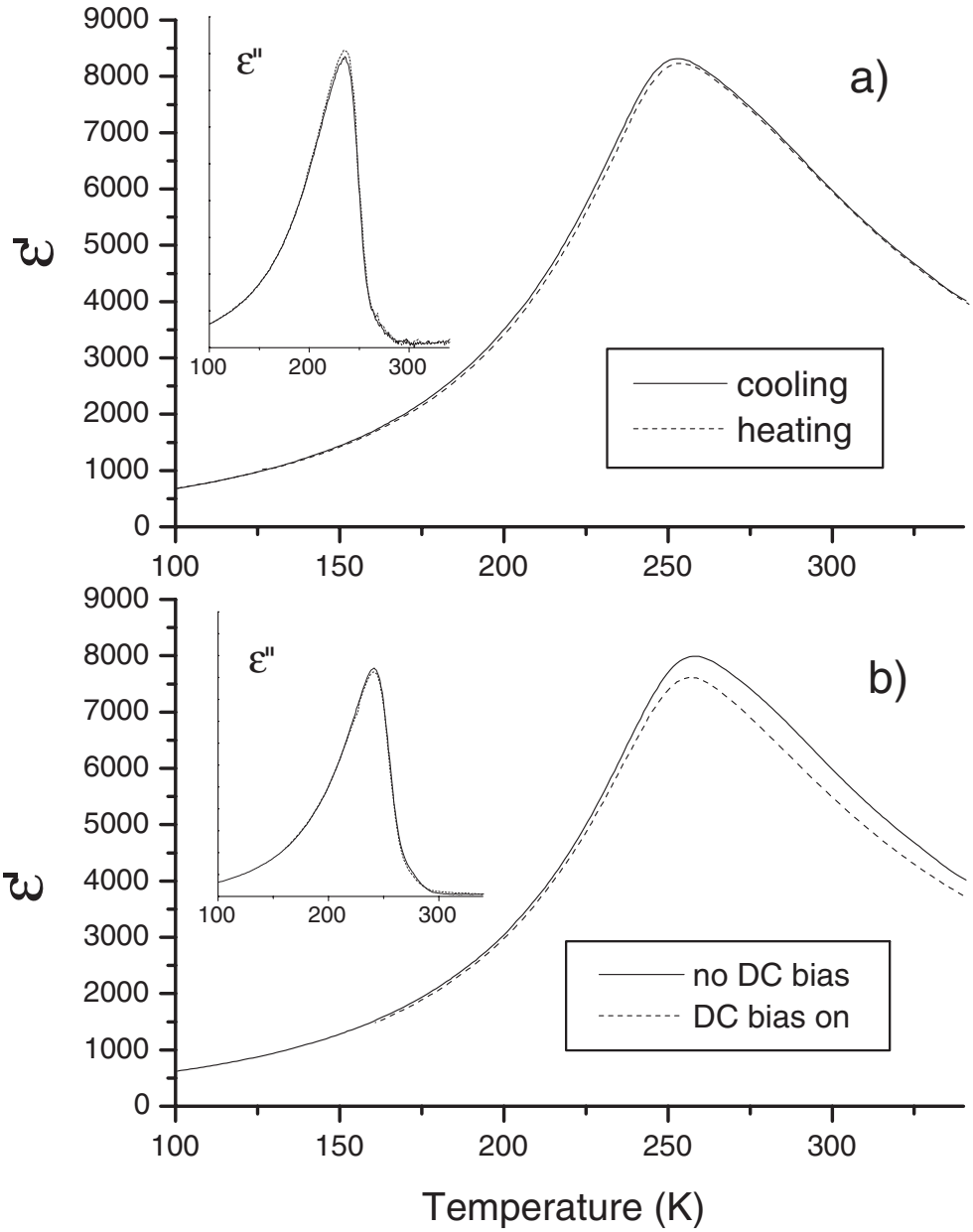

Figure 5. (a) The real part of the complex dielectric constant of PST measured at 1 kHz during cooling (solid line) and heating (dotted line) processes as functions of temperature. (The inset shows the corresponding imaginary parts.) (b) The real part of the complex dielectric constant of PST with no DC bias field (solid line) and with a DC bias field of 400 V cm^{-1} (dotted line) measured at 19.6 kHz during the cooling process as functions of temperature. (The inset shows the corresponding imaginary parts.)

decreasing frequency, which is a quite similar result to that for PMN [6]. We can also see small humps at around 265 K, which might be related to the weak dielectric anomaly observed in the linear dielectric susceptibility (see figure 6(b)). The temperatures of the maxima of P_3 can be

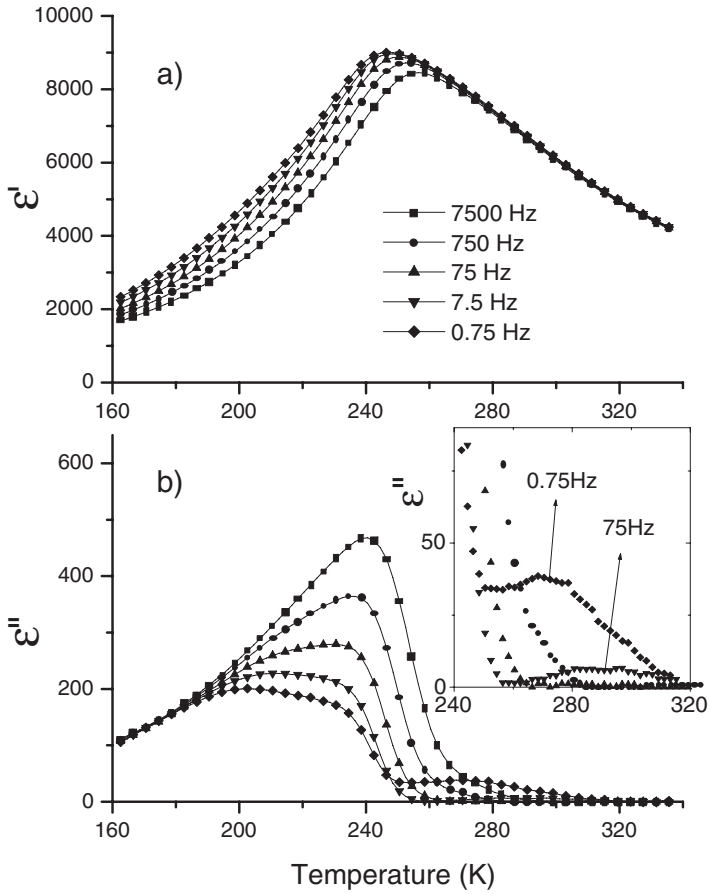

Figure 6. The real part (a) and imaginary part (b) of the complex dielectric constant of PST along ⟨100⟩ at several frequencies between 0.75 Hz and 7500 Hz as functions of temperature. (The inset shows the imaginary part extended to reveal the additional dielectric dispersion.)

fitted by the Vogel–Fulcher law, as shown in figure 7(b), resulting in $\tau_0(1/\omega_0) = 5.0 \times 10^{-8}$ s, $E = 172 \pm 55$ K and $T_f = 224 \pm 2$ K. (As can be seen below, the temperatures of the maxima of $|P_3|$ and $|P_3'|$ at the same frequency are coincident with each other within experimental error.) The freezing temperature $T_f(3\omega)$ (=224 K) obtained from this fit is quite similar to that of the linear dielectric response, $T_f(\omega) = 229$ K. However, other fitting parameters show large differences, and we have no explanation for these differences at present. It might be due to the small frequency range (only three decades) used in the fitting process.

We decomposed the third-harmonic dielectric response into the real and imaginary parts, which are shown in figure 8. The amplitudes of both components are about one order of magnitude smaller than those for PMN [13]. The overall shape of the real part ($-P_3'$) is similar to the absolute value of P_3 in figure 7(a), and the imaginary part shows a distinct nonmonotonic behaviour above 250 K. This well-developed dip can be partly ascribed to the higher-order polarization harmonics; this was supported by the fact that this dip could be enhanced with the increase of the probe amplitude in PMN [13]. However, our data for $-P_3''$ show much wider and deeper minima than those for PMN as can be seen in figure 8(b). One reason may be the relatively poor data condition, with a low signal-to-noise ratio in the high-temperature

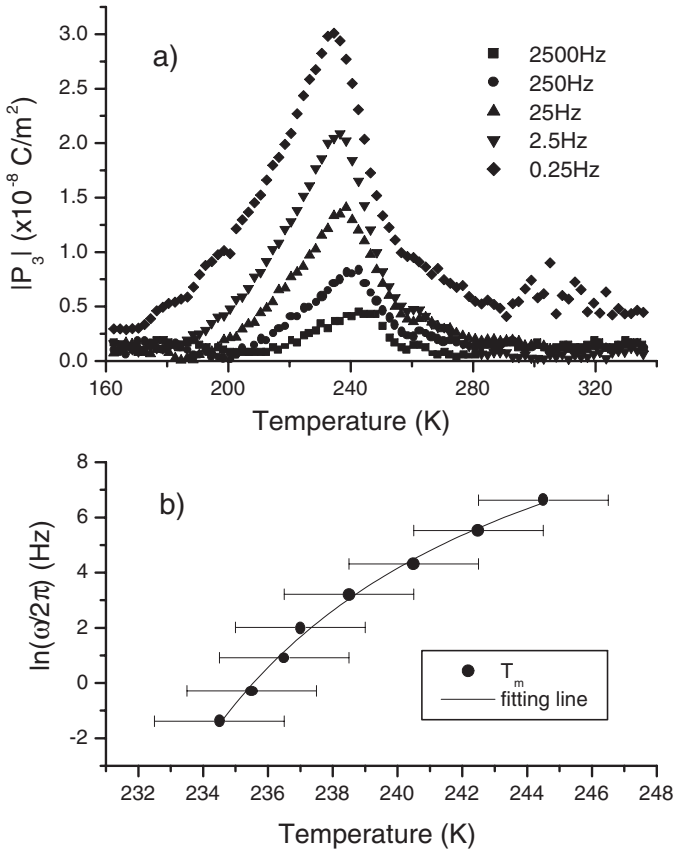

Figure 7. (a) The absolute value of the third-harmonic nonlinear response of PST along the ⟨100⟩ axis measured at several frequencies. (b) The result of fitting the peak temperatures of (a) with the Vogel–Fulcher relation (equation (1)) with typical error bars.

range. Another possible origin may be the additional contribution to the linear and nonlinear dielectric responses, as can be seen in figure 6.

The spherical random-bond–random-field (SRBRF) model [9] puts stress on the nonlinear dielectric constant—in particular, on a_3 ($=\varepsilon_3/\varepsilon_1^4$). According to this model, a_3, in the absence of external fields and random fields, shows diverging behaviour at the freezing temperature while it shows a sharp peak in the presence of weak random fields at a similar temperature. Due to the dynamic nature of the conventional dielectric spectroscopy and the corresponding dielectric dispersion, it would be impossible to observe the sharp peak of the static response at the freezing temperature. Only the high-temperature tail of the peak and a minimum which signals a crossover from the 'glasslike' behaviour in the low-temperature range to the 'paraelectriclike' behaviour in the high-temperature range were observed in PMN and PLZT(9/65/35) relaxors [11]. These experimental results were suggested as strong evidence for a transition to the glassy state and against a transition to the ferroelectric nanodomain state driven by quenched random fields.

In figure 9(a), we have plotted a_3 for PST. a_3 in the high-temperature range is affected by the additional relaxation process mentioned above and shows a weak frequency dispersion. Although we cannot see a monotonically decreasing behaviour in the high-temperature range

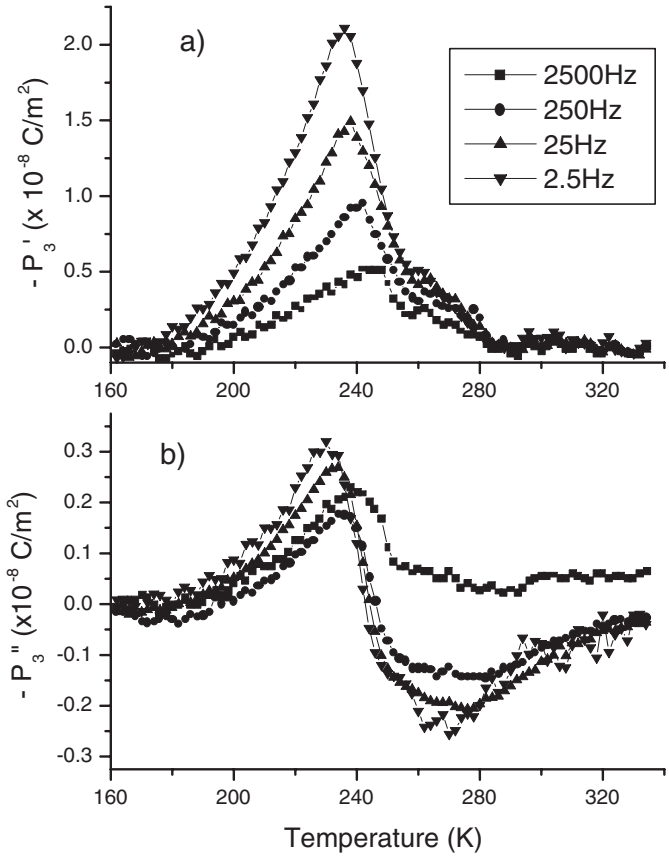

Figure 8. The real part (a) and imaginary part (b) of the complex third-harmonic dielectric response of PST along the ⟨100⟩ axis shown at several frequencies as functions of temperature.

with decreasing temperature, we can see a weak minimum at about 257 K as is indicated by an arrow in the inset of figure 9(a). Below this temperature, a_3 increases with decreasing temperature and shows a large frequency dispersion at the freezing temperature, which is similar to the result for PMN [11]. Since a_3 for PST shows both a minimum and a strong increase at lower temperatures, this result itself seems to be consistent with the predictions of the SRBRF model.

Very recently, Glazounov and Tagantsev proposed a phenomenological model for the dynamic nonlinear response of relaxor ferroelectrics [13]. In this model the free energy of the centrosymmetric relaxor system is expressed by a series expansion in terms of the macroscopic polarization as $G = (\alpha/2)P^2 + (\beta/4)P^4 + \cdots$, where α and β are assumed to be temperature-dependent coefficients. The nonlinear properties are controlled by the term βP^4 if the higher-order terms are omitted. Based on a single-relaxation-time assumption, an equation of motion and the equations for the polarization response can be obtained by utilizing the Landau–Khalatnikov equation [32]. From the expression obtained for $P_3'(=-(\beta/4)[\varepsilon_l'^3(\omega)\varepsilon_l'(3\omega)]\varepsilon_0^4 E_m^3)$, where $\varepsilon_l = \varepsilon_l' - \mathrm{i}\varepsilon_l''$ and E_m are the complex linear dielectric permittivity and the sinusoidal probe amplitude, respectively, it is clear that the coefficient β is proportional to a_3 in the static limit of vanishing frequency and is thus interpreted as a true static nonlinear coefficient [13]. In contrast to the prediction of the SRBRF model, β showed

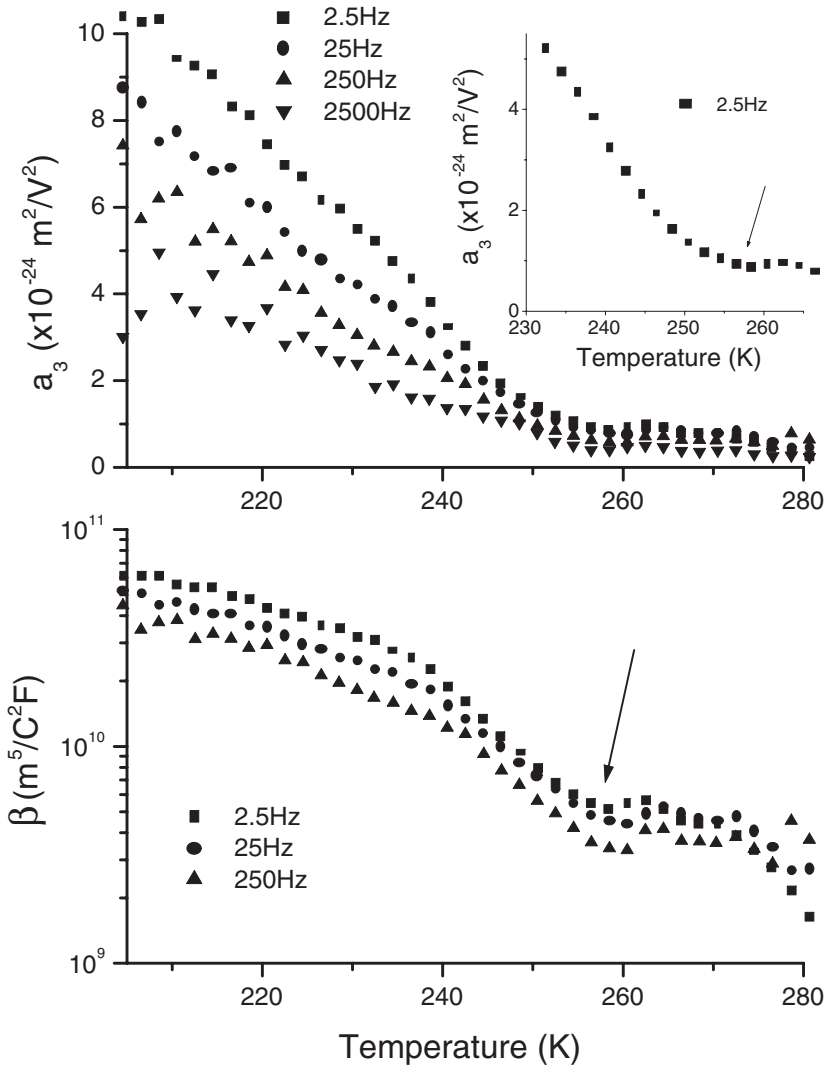

Figure 9. (a) The temperature dependence of the dielectric nonlinearity a_3 obtained at several frequencies in PST. The inset shows the result obtained at 2.5 Hz which reveals a weak dip at about 257 K as indicated by an arrow. (b) The temperature dependence of the nonlinear coefficient β at several frequencies calculated within the phenomenological model from the results on the third harmonics, P_3', and linear permittivity, ε_1'. A dip at about 257 K is indicated by an arrow.

no maximum near the freezing temperature but continued to increase monotonically in the temperature range of the measurement in the case of PMN [13].

We calculated β for PST using the measured linear and nonlinear dielectric constants, as shown in figure 9(b). For the same reason as for a_3, the data above 265 K are scattered owing to an additional relaxation process and a relatively poor data condition. Below this temperature, β shows a minimum at about 257 K and increases monotonically with decreasing temperature. Although it shows a frequency dependence, which can be partly ascribed to the higher-order harmonics [13], the dependence is relatively small compared to the case for a_3 shown in figure 9(a). Similarly to the case for PMN, β for PST shows no maximum near the

freezing temperature (∼229 K), which is not consistent with the theoretical prediction of the SRBRF model for a_3 if β can be considered to reflect the true static nonlinear susceptibility. From both the analysis represented by figure 9 and its comparison with the results for PMN [11, 13], we can say that the dynamical property of the nonlinear response and the quasistatic nature extracted using the phenomenological model [13] for disordered PST single crystal are quite similar to those for PMN. However, since the above model is a phenomenological one and there is no microscopic model which can explain the properties of the linear and nonlinear dielectric susceptibilities of relaxors at both the static and the dynamic level, the physical meaning of β and its inconsistency with the prediction of the SRBRF model should be examined in more detail in further work.

4. Conclusions

Linear and nonlinear dielectric constants were measured for the disordered lead scandium tantalate single crystal. The linear dielectric constant showed typical relaxor behaviours with the dielectric maxima satisfying the Vogel–Fulcher relation without any spontaneous relaxor–ferroelectric transition, which is consistent with the previous results on single-crystal PST samples [14, 17]. We found an additional weak dielectric dispersion, which is significant only at low frequencies, in the high-temperature range. The third-harmonic nonlinear polarization response was measured to examine the two quantities a_3 ($=\varepsilon_3/\varepsilon_1^4$) of the SRBRF model [9–11] and the nonlinear coefficient β of the recently proposed phenomenological model [13]. Both quantities showed minima at about 257 K, which is consistent with the theoretical prediction of the SRBRF model. However, the nonlinear coefficient β, which was interpreted as a true static nonlinear coefficient proportional to a_3, did not show the maximum at the freezing temperature predicted by the SRBRF model, which is similar to the case for PMN.

Acknowledgments

This work was supported by the Marubun Research Promotion Foundation and the University of Tsukuba Research Projects.

References

[1] Cross L E 1987 *Ferroelectrics* **7** 241
[2] Burns G and Dacol F H 1990 *Ferroelectrics* **104** 25
[3] Jiang F M and Kojima S 2000 *Phys. Rev.* B **62** 8572
[4] Viehland D, Jang S J, Cross L E and Wuttig M 1992 *Phys. Rev.* B **46** 8003
[5] Colla E V, Koroleva E Y, Okuneva N M and Vakhrushev S B 1995 *Phys. Rev. Lett* **74** 1681
[6] Levstik A, Kutnjak Z, Filipič C and Pirc R 1998 *Phys. Rev.* B **57** 11 204
[7] Westphal V, Kleemann W and Glinchuk M D 1992 *Phys. Rev. Lett.* **68** 847
[8] Tagantsev A K and Glazounov A E 1998 *Phys. Rev.* B **57** 18
[9] Pirc R and Blinc R 1999 *Phys. Rev.* B **60** 13 470
[10] Blinc R, Dolinšek J, Gregorovič A, Zalar B, Filipič C, Kutnjak Z, Levstik A and Pirc R 1999 *Phys. Rev. Lett.* **83** 424
[11] Bobnar V, Kutnjak Z, Pirc R, Blinc R and Levstik A 2000 *Phys. Rev. Lett.* **84** 5892
[12] Tagantsev A K and Glazounov A E 1998 *Phase Transitions* **65** 117
[13] Glazounov A E and Tagantsev A K 2000 *Phys. Rev. Lett.* **85** 2192
[14] Setter N and Cross L E 1980 *J. Appl. Phys.* **51** 4356
[15] Wang H-C and Schulze W A 1990 *J. Am. Ceram. Soc.* **73** 1228
[16] Chu F, Setter N and Tagantsev A K 1993 *J. Appl. Phys.* **74** 5129
[17] Viehland D and Li J-F 1994 *J. Appl. Phys.* **75** 1705

[18] Chu F, Setter N, Elissalde C and Ravez J 1996 *Mater. Sci. Eng.* B **38** 171
[19] Siny I G and Boulesteix C 1989 *Ferroelectrics* **96** 119
[20] Gvasaliya S N, Lushnikov S G, Siny I G, Sashin I L, Shaplygina T A and Blinc R 2000 *Physica* B **276–278** 485
[21] Dmowski W, Akbas M K, Davies P K and Egami T 2000 *J. Phys. Chem. Solids* **61** 229
[22] Chu F, Reaney I M and Setter N 1995 *J. Am. Ceram. Soc.* **78** 1947
[23] Blinc R, Gregorovič A, Zalar B, Pirc R and Lushnikov S G 2000 *Phys. Rev.* B **61** 253
[24] Chu F, Reaney I M and Setter N 1995 *J. Appl. Phys.* **77** 1671
[25] Kim B-G and Kim J-J 1999 *Phys. Rev.* B **59** 13 509
[26] Maglione M, Böhmer R, Loidl A and Höchli U T 1989 *Phys. Rev.* B **40** 11 441
[27] Elissalde C, Ravez J and Gaucher P 1992 *Mater. Sci. Eng.* B **13** 327
[28] Ko J-H, Jiang F M, Kojima S, Shaplygina T A and Lushnikov S G 2001 to be submitted
[29] Bovtun V, Porokhonskyy V, Petzelt J, Savinov M, Endal J, Elissalde C and Malibert C 2000 *Ferroelectrics* **238** 17
[30] Randall C A, Markgraf S A, Bhalla A S and Baba-Kishi K 1989 *Phys. Rev.* B **40** 413
[31] Takesue N, Fujii Y, Ichihara M and Chen H 1999 *Phys. Rev. Lett.* **82** 3709
[32] Orihara H, Fukase A, Izumi S and Ishibashi Y 1993 *Ferroelectrics* **147** 411
[33] Reaney I M, Petzelt J, Voitsekhovskii V V, Chu F and Setter N 1994 *J. Appl. Phys.* **76** 2086
[34] Petzelt J, Buixaderas E and Pronin A V 1998 *Mater. Sci. Eng.* B **55** 86